Int. J. Electrochem. Sci., 15 **(2020)** 4789 – 4797, doi: 10.20964/2020.05.87

International Journal of
ELECTROCHEMICAL
SCIENCE
www.electrochemsci.org

Short Communication

Facile synthesis of hollow Fe_3O_4 nanospheres and their application as drug delivery carrier and anode for lithium-ion batteries

Haonan Zhang[1,2,3,#], *Bin Wang*[1,2,3,4,#], *Tongguo Si*[1,2,3,*]

[1] Department of Interventional Therapy, Tianjin Medical University Cancer Institute and Hospital, National Clinical Research Center for Cancer,Tianjin, 300060, PR China
[2] Key Laboratory of Cancer Prevention and Therapy, Tianjin, 300060, PR China
[3] Tianjin's Clinical Research Center for Cancer,Tianjin, 300060, PR China
[4] Intervention therapy department, Tianjin Huanhu Hospital, Tianjin Key Laboratory of Cerebral Vascular and Neurodegenerative Diseases, Tianjin 300350, PR China
[*]E-mail: drsitg@163.com
# The authors contributed equally to this work

Received: 1 November 2019 / *Accepted:* 15 January 2020 / *Published:* 10 April 2020

Multi-functional materials that can be used in a variety of different applications have attracted significant research interest. Herein, we report a facile method for preparing hollow Fe_3O_4 nanospheres with good magnetic properties and substantial surface areas. The as-prepared hollow Fe_3O_4 nanospheres can be used as drug carriers. The chemotherapeutic agent oxorubicin hydrochloride (DOX) was used to study the controlled release behavior of the hollow Fe_3O_4 nanospheres. The drug release curves showed a high DOX loading efficiency and pH-dependent drug release. Less DOX was released at pH 7.4 compared to pH 6.2 due to the protonation of DOX in acidic environments, implying stable release rates. Furthermore, using Fe_3O_4 as an anode in lithium-ion batteries delivers a reversible capacity of 631 mAh g^{-1} at 2 A g^{-1}, which can be attributed to the specific structure of the hollow Fe_3O_4 nanospheres. Hence, this study provides a novel nano platform based on magnetic targeting and new pH-responsive drug delivery system for cancer treatment.

Keywords: Fe_3O_4 nanospheres, Drug carrier, Lithium ion battery, Anode

1. INTRODUCTION

Due to the rapid advancement of modern society, metal oxides have been employed in many developing industrial applications, such as in electronic devices, medical treatments and chemical catalysis [1-3]. Fe_3O_4 is an important metal oxide that is particularly attractive due to its outstanding chemical stability, excellent bio-compatibility, and low toxicity [4-5]. Fe_3O_4 has been widely used in

biomedicine, energy storage media and magnetic resonance imaging [6-7]. It is well known that the composition and crystal structure of nanomaterials are key to their physical and chemical properties [8-9]. Thus, developing fabrication methods that control the composition and morphology of iron oxide is a significant challenge.

Currently, the development of new and innovative drug delivery systems plays an important role to medicine and health care. Recently, hollow nanomaterials with strong adsorptivity have been widely used for drug delivery due to their large surface areas and rich porous structures [10-12]. Magnetic nanoparticles possess several advantageous properties, including biocompatibility and super-paramagnetism. These materials can be used as MRI agents and also as magnet-driven drug delivery systems. Among of all the possible candidates for these applications, Fe_3O_4 nanoparticles are considered to be an attractive and promising material because of their high biocompatibility, used in magnetic resonance imaging, potential for targeted drug delivery, easily synthesised and have low cost and [13]. Many Fe_3O_4-based hybrids, such as carbon-coated Fe_3O_4, have been designed and investigated as drug carriers [14-15]. However, the preparation of Fe_3O_4-based hybrids has some shortcomings, such as the typical long preparation time, the formation of by-products and the complexity of the required procedures [16].

Herein, we report the preparation of hollow Fe_3O_4 nanospheres using a facile hydrothermal method. The crystalline phase, topography and magnetic properties of the hollow Fe_3O_4 nanospheres were determined. In order to investigate their use as a drug delivery system, hollow Fe_3O_4 nanospheres were used as a drug carrier for doxorubicin hydrochloride (DOX). In addition, we tested the application of the hollow Fe_3O_4 nanospheres as electrode materials for enhanced lithium storage performance. It is well known that the large volume change in Fe_3O_4 caused by delithiation/lithiation during the charge and discharge processes often leads to poor cycling performance and decreasing capacity. In this study, the synthesized hollow Fe_3O_4 nanospheres alleviated the local tension stress responsible for volume changes during the change-discharge process. The well-designed Fe_3O_4 nanosphere anode exhibits a reversible discharge capacity of 743 mAh g^{-1} at a current density of 0.2 A g^{-1} over 100 cycles. The design approach in this work, of using a spherical structure, provides a promising strategy for high performance lithium-ion batteries.

2. MATERIALS AND METHODS

2.1. Preparation of the materials

The hollow Fe_3O_4 nanospheres were prepared using a simple hydrothermal procedure. First, a solution of 0.34 g $Fe(NO_3)_3 \cdot 6H_2O$, 15 mL glycerol and 105 mL isopropanol was mixed via stirring for 10 min. Then 2 mL of deionized water was added to the above solution, followed by stirring for 20 min. Then the homogeneous solution was poured into a Teflon stainless steel autoclave and heated in an electric oven for 11 h at 200 °C. The reaction mixture was cooled to the room temperature and the solid products were removed by centrifugation, washed and dried for 24 h at 80 °C. Finally, the products were heated at 370 °C under nitrogen atmosphere for 2 h to obtain the hollow Fe_3O_4 nanospheres.

2.2. Characterization

X-ray diffraction (XRD, D8 Focus, Bruker) was performed with Cu Kα radiation in the 10° to 90° range. The morphologies of the sample were determined using transmission electron microscopy (TEM, JEM2100F, JEOL) and scanning electron microscopy (SEM, Hitachi, S-4800). The magnetic properties were measured using a vibrating sample magnetometer (VSM) in a magnetic field range of -2000 Oe to 2000 Oe at 300 K. The pore size distribution and specific surface area were determined by Brunauer-Emmett-Teller analysis (BET, Micromeritics ASAP2020).

2.3. Drug loading and release

The drug loading was carried out by mixing 4 mg of a solution of the anti-cancer drug DOX with 10 mg hollow Fe_3O_4 nanospheres. The mixture was then centrifuged to remove unbound DOX. The resulting mixture was homogeneous and was re-suspended in phosphate buffered saline (PBS) with various pH values (pH = 6.2 or 7.4) under gentle shaking at 37 °C. The drug loading concentration (DLC) of DOX loaded into the hollow Fe_3O_4 nanospheres was calculated using the following formula: $DLC(\%)=M_n/M_0*100\%$, where M_n is the gross mass of DOX released from the DOX loaded into the hollow Fe_3O_4 nanospheres, and M_0 is the original mass of DOX used for the drug loading.

2.4. Electrochemical experiments

The electrochemical performance of the hollow Fe_3O_4 nanospheres was measured using coin-type cells (CR2025). A slurry was formed by mixing the active material, Fe_3O_4, with polyvinylidene fluoride as the binder and acetylene black as the conducting agent with a ratio of 8:1:1 in 1-methyl-2-pyrrolidinone. The slurry was uniformly pressed on Cu foil and dried at 60 °C for 12 h. The electrolyte was 1 M $LiPF_6$ dissolved in a 1:1:1 mixture of Ethylene carbonate/Diethyl carbonate/Dimethyl carbonate(EC/DEC/DMC). The coin-type cells were assembled in a glove box (MBraun) under argon (99.9995%, purity) atmosphere. The galvanostatic charge/discharge curves and cyclic voltammetry (CV) were determined using a multichannel battery tester (BT-2000, Arbin Instruments) and an electrochemical workstation (VMP3, Biologic), respectively, in the 0.01 to 3.0 V potential window.

2.5. Cell cytotoxicity experiments

The cytotoxicity of the hollow Fe_3O_4 nanospheres against HeLa cells was studied by CCK-8. Hela cells were incubated in 96-well plates (5×10^3 cells per well) under 5% CO_2 at 37 °C for 24 h. Then, the cells were incubated with 100 μL of fresh medium containing various concentrations of hollow Fe_3O_4 nanospheres (50, 100, 200, 400, and 800 μg/mL) for another 24 h. A control experiment containing no hollow Fe_3O_4 nanospheres was performed at the same time. Afterwards, 10 μL of a CCK-8 solution was added to each well and further incubated for 4 h at 37 °C under 5% CO_2. The optical density (OD) was measured using an ELISA reader. The relative cell viability (*CV*, %) of the hollow Fe_3O_4 nanospheres was calculated using the following equation:

$$CV(\%) = \frac{OD(e) - OD(b)}{OD(c) - OD(b)} \times 100\%$$

where *OD(e)*, *OD(c)*, and *OD(b)* represent the OD values of the experimental group, the control group and 100 μL of medium containing 10 μL CCK-8, respectively.

3. RESULTS AND DISCUSSION

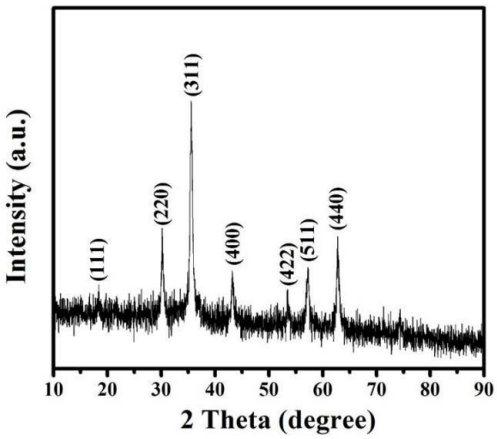

Figure 1. XRD pattern of the hollow Fe_3O_4 nanospheres.

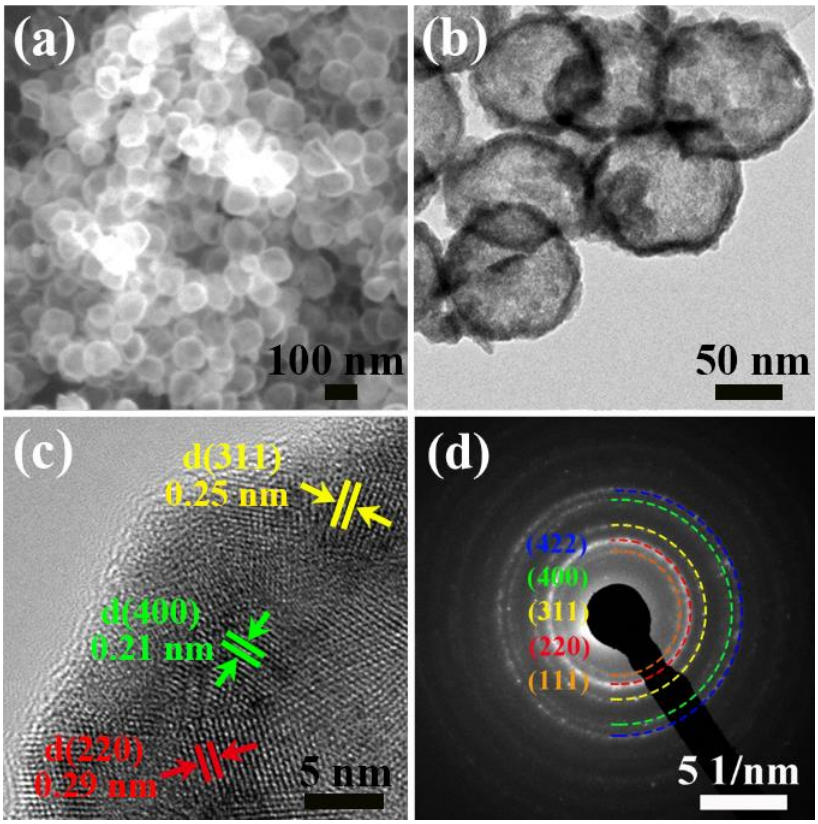

Figure 2. (a) SEM image, (b) TEM image, (c) HRTEM image and (d) SAED patterns of the hollow Fe_3O_4 nanospheres.

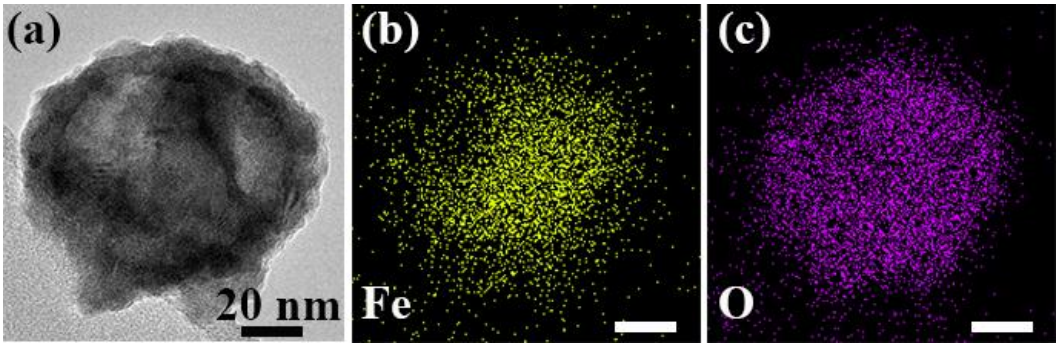

Figure 3. (a) TEM image of a single Fe_3O_4 nanosphere and the corresponding EDX mapping images for (b) Fe and (c) O.

The XRD pattern of the hollow Fe_3O_4 nanospheres is shown in Figure 1. The intrinsic diffraction peaks at 2θ values of 18.3°, 30.2°, 35.5°, 43.4°, 53.6°, 57.1° and 63.1° correspond to the (111), (220), (311), (400), (422), (511) and (440) lattice planes of Fe_3O_4, consistent with the recorded values for Fe_3O_4 (PDF#65-3107). These results confirm the successful preparation of the hollow Fe_3O_4 nanospheres.

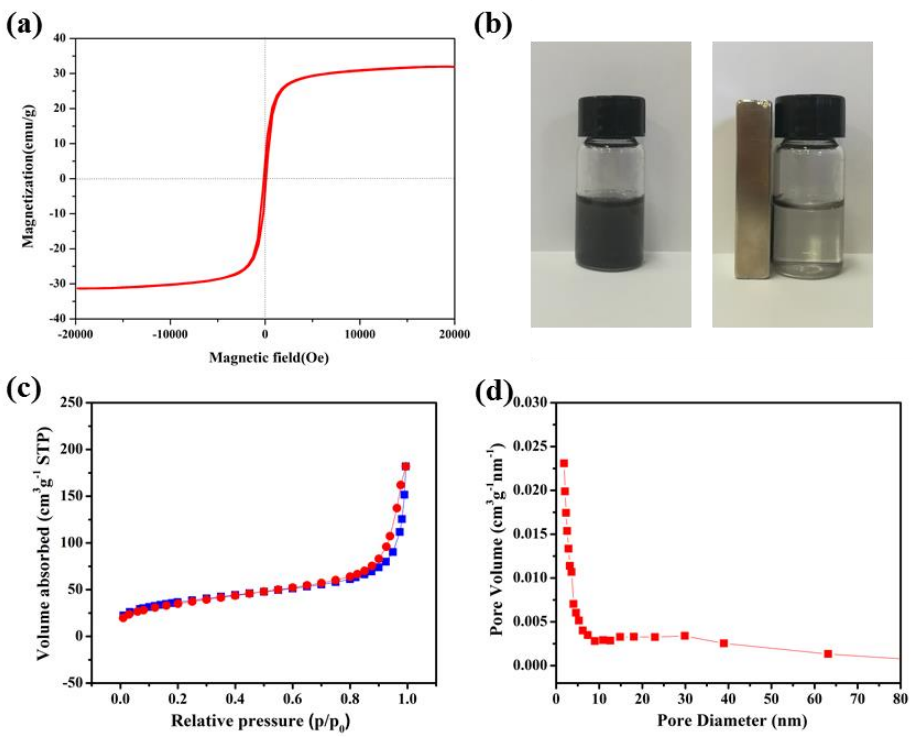

Figure 4. (a) Magnetic hysteresis loop, (b) demonstration of the magnetic separation of the nanospheres, (c) nitrogen adsorption-desorption isotherms and (d) pore-size distribution of the hollow Fe_3O_4 nanospheres.

The morphology of the hollow Fe_3O_4 nanospheres was characterized by SEM and TEM. As shown in Figure 2(a), the synthesized hollow Fe_3O_4 nanospheres were monodisperse, with an average diameter of 100 nm, indicating their successful preparation using a facile hydrothermal method. The

Fe_3O_4 nanospheres were identified to be hollow nanospheres based on the results in Figure 2(b). The lattice fringes of the hollow Fe_3O_4 nanospheres were clearly observed in the HRTEM image. As illustrated in Figure 2(c), interplanar spacings of 0.21 nm, 0.25 nm and 0.29 nm were attributed to the (400), (311) and (220) planes of the hollow Fe_3O_4 nanospheres, respectively. The selected area electron diffraction (SAED) patterns in Figure 2(d) also exhibited distinct polycrystalline diffraction rings, consistent with the XRD results. The EDX mapping of a single Fe_3O_4 nanosphere (Figure 3) indicated that the Fe_3O_4 nanosphere contained a homogeneously distribution of Fe and O.

The magnetic properties of the hollow Fe_3O_4 nanosphere were measured in a magnetic field range of -2000 Oe to 2000 Oe at 300 K using a VSM. As shown in Figure 4(a), the evaluated magnetization saturation (Ms) value was 31.1 emu/g and the magnetic hysteresis loop was an S-type curve, which shows no hysteresis. In addition, the cross section of the magnetization curve was close to zero, indicating that there was almost no remanence or coercivity and that the hollow Fe_3O_4 nanospheres exhibited super paramagnetism [17-18]. The hollow Fe_3O_4 nanospheres could be separated using magnetism, as presented in Figure 4(b). The magnetic hollow Fe_3O_4 nanospheres were attracted to the magnet, indicating that the material could be used to carry drugs to magnetically targeted positions in addition to using a magnetic field for separation. The nitrogen adsorption-desorption isotherms shown in Figure 4(c) are type-IV, indicating a mesoporous material, which is advantageous for drug loading. The BET specific surface area was 131.7 $m^2 g^{-1}$. In addition, the pore size distribution of 5.2 nm for the nanospheres is shown in Figure 4(d). The high BET specific surface area is also advantageous for drug loading.

To investigate the electrochemical performance of the hollow Fe_3O_4 nanospheres, the galvanostatic charge/discharge, cycling and rate capabilities were measured in the range of 0.01 to 3.0 V. Based on the results in Figure 5(a), the initial discharge capacity was 1137 mAh g^{-1}. The presence of two potential plateaus at 0.9 V in the first discharge curve could be attributed to the formation of the solid electrolyte interface (SEI) and to the lithiation reaction of Fe_3O_4, respectively [22]. In the subsequent cycles, the potential plateau due to SEI formation disappeared. The Fe_3O_4 anode showed a reversible discharge capacity of 743 mAh g^{-1} after 100 cycles, indicating superior cycling stability (Figure 5(b)). In addition, the rate capability is assessed in Figure 5(c). The results show that the Fe_3O_4 anode retained a lower discharge capacity of 631 mAh g^{-1} at 2 A g^{-1}. When the current density was returned to 0.2 A g^{-1}, it still exhibited a high discharge capacity of 905 mAh g^{-1}.

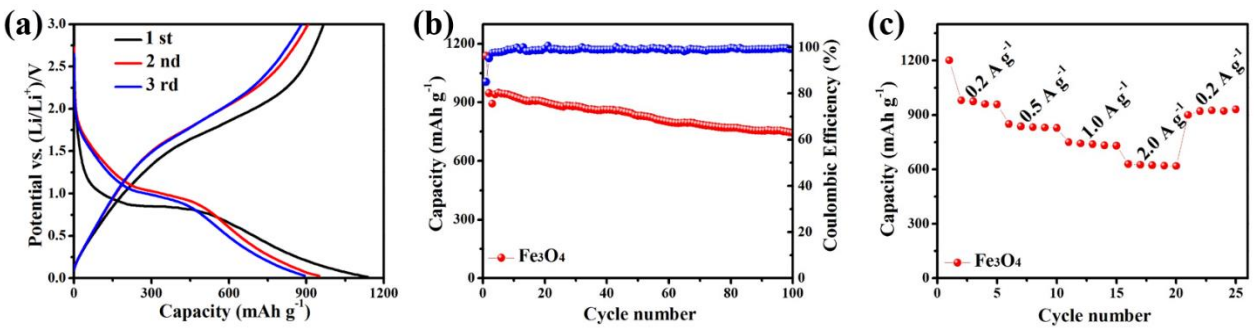

Figure 5. (a) Charge/discharge curves, (b) cycling performance at 0.2 A g^{-1} and (c) rate capabilities of the hollow Fe_3O_4 nanospheres.

To clearly compare the differences between the novel Fe_3O_4 anode and conventional Fe_3O_4 composite electrodes in LIBs, the results from some related work are summarized in Table 1 below. As shown in Table 1, the Fe_3O_4 nanospheres fabricated in this work showed an excellent rate performance of 631 mAh g^{-1} (at 2 A g^{-1}), which is superior to previously reported composite Fe_3O_4 electrodes.

Table 1. Comparison of the electrochemical performance of previous reports with our work.

Materials	Initial capacity (mAh g^{-1}, at n C)	Final capacity (mAh g^{-1}, after n cycles)	High rate performance (mAh g^{-1}, at n C)	Ref.
Fe_3O_4@C	667 (0.1 A g^{-1})	660 (100th)	570 (1.5 A g^{-1})	[14]
Fe_3O_4@C	600 (1 C)	720 (150th)	400 (8 A g^{-1})	[24]
Fe_3O_4@C nanoparticles	925 (0.2 A g^{-1})	690 (60th)	300 (10 C)	[25]
CGFE	1307 (0.1 A g^{-1})	812.9 (190th)	283 (1.6 A g^{-1})	[26]
Fe_3O_4 nanospheres	1137 (0.2 A g^{-1})	743 (100th)	631 (2 A g^{-1})	This work

The drug release behavior of the DOX-loaded hollow Fe_3O_4 nanospheres was studied by examining the sustained release for 100 h at 37 °C at pH=7.4, in a physiologically relevant environment, and at pH=6.2, in an acidic environment (Figure 6).

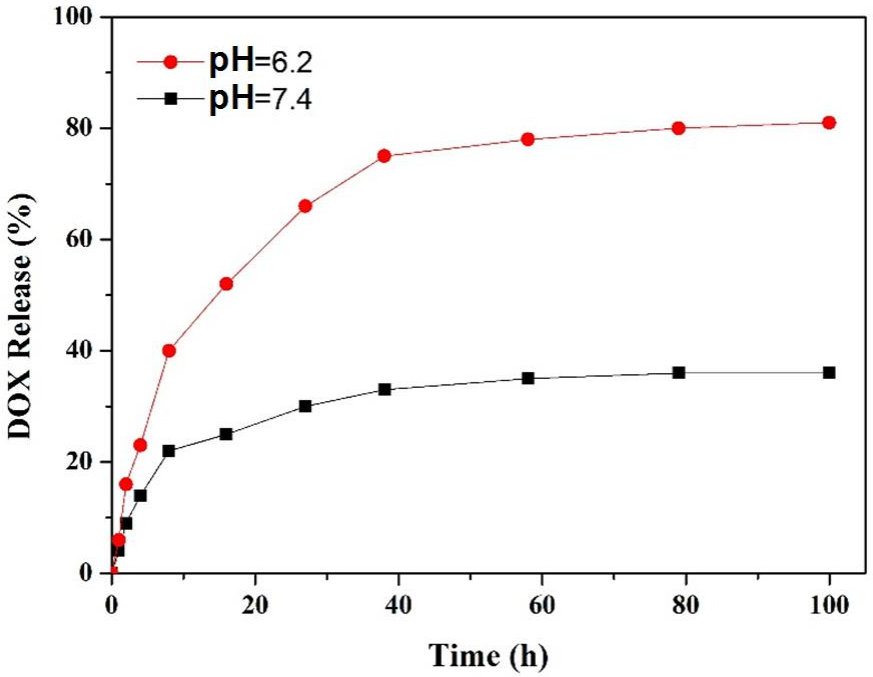

Figure 6. Drug-release kinetic curves obtained at pH = 6.2 (red) and pH = 7.4 (black) using the hollow Fe_3O_4 nanospheres.

These different pH values represented the drug release behavior under the conditions relevant for drug release at the target locations. Quick release of the drug occurred during the initial stage and thereafter a steady and slow release of the drug was observed. The total amount of DOX released at pH 6.2 was 81%, which is much higher than the amount released at pH 7.4 (36%). This result is consistent

with the insolubility of DOX in a physiological environment and favors the use of these nanospheres as responsive drug carriers, so that a higher amount of the drug is released after the drug-loaded hollow Fe_3O_4 nanospheres reach the target location. Thus, the DOX-loaded hollow Fe_3O_4 nanospheres showed pH-responsive drug release behavior. In addition, the nonlinear relationship between the release rate and time indicated that the hollow Fe_3O_4 nanospheres could provide constant release of the drug and therefore act as a protective shell in biological media for potential cancer therapies [19-21].

In addition, the cytocompatibility of the hollow Fe_3O_4 nanospheres against HeLa cells was performed. Figure 7 shows the cell viability profile. The results revealed that the DOX-loaded hollow Fe_3O_4 nanospheres and free DOX have similar cytotoxicity against Hela cells. In addition, the hollow Fe_3O_4 nanospheres showed high cell viability and good cytocompatibility up to a concentration of 400 μg/mL. Thus, the hollow Fe_3O_4 nanospheres show promise for applications as drug delivery systems because of their good biocompatibility and slow drug release.

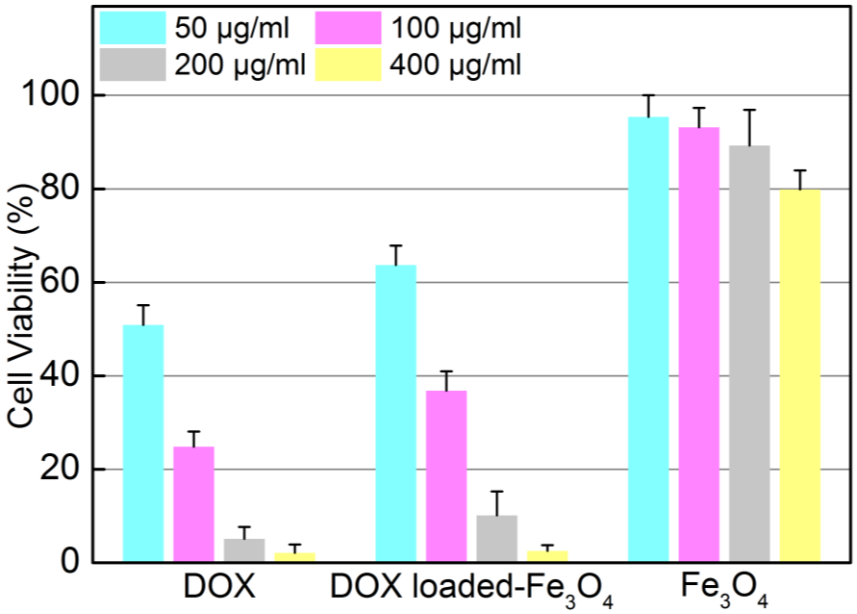

Figure 7. Viability of Hela cells after incubation with different concentrations of DOX, DOX-loaded hollow Fe_3O_4 nanospheres, and hollow Fe_3O_4 nanospheres for 24 h.

4. CONCLUSIONS

In this paper, hollow Fe_3O_4 nanospheres have been synthetized using a facile hydrothermal method. These nanospheres retained their perfect crystalline structure and showed superparamagnetic behavior. When used as a drug carrier, the hollow Fe_3O_4 nanospheres stored a high amount of the drug DOX and showed sustained release behavior. Hence, the hollow Fe_3O_4 nanosphere are suitable drug targeted drug delivery carriers for improved theranostic applications. In addition, lithium-ion battery anodes prepared using the hollow Fe_3O_4 nanospheres delivered good cycling stability and superior rate performance.

CONFLICTS OF INTEREST
The authors declare no conflicts of interest.

References

1. P. Poizot, S. Laruelle, S. Grugeon, L. Dupont and J.M. Tarascon, *Nature,* 407 (2000) 496-499.
2. M. Kundu, G. Karunakaran, S. Kumari, N. Van Minh, E. Kolesnikov, M.V. Gorshenkov and D. Kuznetsov, *J. Alloy Compd.,* 725 (2017) 665-672.
3. X.H. Huang, X.H. Xia, Y.F. Yuan and F. Zhou, *Electrochim. Acta,* 56 (2011) 4960-4965.
4. C.T. Hsieh, C.Y. Lin, Y.F. Chen and J.S. Lin, *Electrochim. Acta,* 111 (2013) 359-365.
5. H. Li, Y. Li, Y. Zhang and C. Zhang, *J. Nanopart. Res.,* 17 (2015) 370.
6. H. Yue, Q. Wang, Z. Shi, C. Ma, Y. Ding, N. Huo, J. Zhang and S. Yang, *Electrochim. Acta,* 180 (2015) 622-628.
7. H.C. Tao, X.L. Yang, L.L. Zhang and S.B. Ni, *J. Electroanal. Chem.,* 739 (2015) 36-42.
8. M. Du, C. Xu, J. Sun and L. Gao, *Electrochim. Acta,* 80 (2012) 302-307.
9. S.M. Abbas, S. Ali, N. Ahmad, N. Ali and S. Abbas, *J. Mater. Sci.,* 48 (2013) 5429-5436.
10. H.P. Li, L.C. Sun, Y. Zhao, T.Z. Tan and Y.G. Zhang, *Electrochim. Acta,* 295 (2019) 822-828.
11. Y. Luqmani, *Med. Prin. Pract., 14 (2005)* 35-48.
12. M.P. Kesavan, G.G. Vinoth Kumar, J. Dhaveethu Raja, K. Anitha, S. Karthikeyan and J. Rajesh, *J. Photochem. Photobiol., B,* 167 (2017) 20-28.
13. B. Dutta, N.G. Shetake, B.K. Barick, K.C. Barick, B.N. Pandey, K.I. Priyadarsini and P.A. Hassan, *Colloids Surf., B,* 162 (2018) 163-171.
14. Y.G. Zhang, Y. Li, H.P. Li, Y. Zhao, F.X. Yin and Z. Bakenov, *Electrochimi. Acta,* 216 (2016) 475-483.
15. L.W. Cheng, M. Ruan, B.F. Zou, Y.Y. Liu and Y.Q. Wang, *Acta Biomater.,* 58 (2017) 432-441.
16. Y. Zhao, Y.G. Zhang, Z. Bakenov and P. Chen, *Solid State Ionics,* 234 (2013) 40-45.
17. J. Zhang and R.D.K. Misra, *Acta Biomater.,* 3 (2007) 838–850.
18. Q. Yuan, R. Venkatasubramanian, S. Hein and R.D.K. Misra, *Acta Biomater.,* 4 (2008) 1024–1037.
19. J. Chen, Z. Guo, H. Wang, M. Gong, X. Kong, P. Xia and Q. Chen, *Biomaterials,* 34 (2013) 571–581.
20. G. Mao, W. Yang, F. Bu, D. Jiang, Z. Zhao, Q. Zhang, Q. Fang and J. Jiang, *J. Mater. Chem. B,* 2 (2014) 4481–4488.
21. W. Qian, D. Sun, R. Zhu, X. Du, H. Liu and S. Wang, *Int. J. Nanomed.,* 7 (2012) 5781–5792.
22. J. Yan, G. Wang, H. Wang, Z. Zhang, X. Ruan, W. Zhao, J. Yun and M. Xu, *J. Nanopart. Res.,* 17 (2015) 1-10.
23. S. Gu and A. Zhu, *J. Alloy Compd.,* 813 (2020) 152160.
24. Y,B. Su, F,X. Wang, Z. Jian, R.A. Tong, S.K. Chong, W. Wang, C.A. Wang and C.F. Chen, *J. Mater. Chem. A,* 7 (2019) 20899-20904.
25. Z.J. Cao and X.B. Ma, *J. Alloy Compd.,* 815 (2020) 152542.
26. P. Salimi, O. Norouzi and S.E.M. Pourhosseini, *J. Alloy Compd.,* 786 (2019) 930-937.
27. L. Li, H.L. Wang, Z.J. Xie, C.H. An, G.X. Jiang and Y.J. Wang, *J. Alloy Compd.,* 815 (2020) 152337.